Advantages of zinc isotopes as a new dietary proxy in marine ecology

Jeremy McCormack (jeremy_mccormack@eva.mpg.de)
Max Planck Institute for Evolutionary Anthropology https://orcid.org/0000-0002-5995-877X
Paul Szpak
Trent University
Nicolas Bourgon
Max Planck Institute for Evolutionary Anthropology
Michael P. Richards
Simon Fraser University https://orcid.org/0000-0001-5274-8887
Corrie Hyland
Trent University
Pauline Méjean
Géosciences Environnement Toulouse - Observatoire Midi-Pyrénées
Jean-Jacques Hublin
Max Planck Institute of Evolutionary Anthropology https://orcid.org/0000-0001-6283-8114
Klervia Jaouen
Géosciences Environnement Toulouse - Observatoire Midi-Pyrénées

Article

Keywords: Zinc isotopes, diet, trophic ecology, nitrogen isotopes, Arctic, polar bear, ringed seal

Posted Date: December 2nd, 2020

DOI: https://doi.org/10.21203/rs.3.rs-102358/v1

Version of Record: A version of this preprint was published at Communications Biology on June 3rd, 2021. See the published version at https://doi.org/10.1038/s42003-021-02212-z.

Advantages of zinc isotopes as a new dietary proxy in marine ecology

Jeremy McCormack[a]*, Paul Szpak[b], Nicolas Bourgon[a,c], Michael Richards[d], Corrie Hyland[b], Pauline Méjean[e], Jean-Jacques Hublin[a] and Klervia Jaouen[a,e]

[a]*Department of Human Evolution, Max Planck Institute for Evolutionary Anthropology, 04103, Leipzig, Germany*

[b]*Department of Anthropology, Trent University, Peterborough, ON, K9L 0G2, Canada*

[c]*Applied and Analytical Paleontology, Institute for Geosciences, Johannes Gutenberg-University Mainz, 55099 Mainz, Germany*

[d]*Department of Archaeology, Simon Fraser University, Burnaby, BC, V5A 1S6, Canada*

[e]*Géosciences Environnement Toulouse, UMR 5563, CNRS, Observatoire Midi Pyrénées, 31400 Toulouse, France*

**corresponding author*

Abstract

In marine ecology, dietary interpretations of faunal assemblages often rely on nitrogen isotopes as the main or only applicable trophic level tracer. We investigate geographic variability and trophic level isotopic discrimination factors of a new tracer, bone $^{66}Zn/^{64}Zn$ ratios ($\delta^{66}Zn$ value), and compared it to collagen nitrogen and carbon stable isotope ($\delta^{15}N$ and $\delta^{13}C$) values. Focusing on ringed seals (*Pusa hispida*) and polar bears (*Ursus maritimus*) from multiple Arctic archaeological sites, we investigate trophic interactions between predator and prey over a broad geographic area. All proxies show variability among sites, influenced by the regional food web baselines. However, $\delta^{66}Zn$ shows a significantly higher homogeneity among different sites. We observe a clear trophic spacing for $\delta^{15}N$ and $\delta^{66}Zn$ values in all locations, yet $\delta^{66}Zn$ may more reliably record trophic levels between *U. maritimus* and prey species than $\delta^{15}N$. $\delta^{66}Zn$ analysis allows a more direct dietary comparability between spatially and temporally distinct locations than what is possible by $\delta^{15}N$ and $\delta^{13}C$ analysis alone. When combining all three proxies a more detailed and refined dietary analysis is possible.

Keywords

Zinc isotopes, diet, trophic ecology, nitrogen isotopes, Arctic, polar bear, ringed seal

Main

In ecology, archaeology and palaeontology, accurately reconstructing trophic levels can be challenging. Among others, these reconstructions are required for effective management and conservation strategies[1], understanding changing predator-prey and foraging ecology related to climate change[2] and for the comparison of modern to fossil faunal assemblages[3,4]. Stable isotope analysis is an effective tool for analysing marine food webs, complementary to and often more reliable than non-stable isotope approaches[5]. Bone collagen and soft tissue $\delta^{15}N$ and $\delta^{13}C$ values are the traditional geochemical proxies used for dietary and trophic level reconstructions[6,7,8]. Only recently, studies of the bone's mineral phase (bioapatite) non-traditional isotope systems such as calcium, magnesium and zinc (Zn) have shown potential as palaeodietary proxies in the terrestrial[9,10,11] and marine realm[12,13]. Element and isotope ratios observed in a diagenetically more resistant mineral phase (e.g., enamel) can preserve dietary information beyond the scope of application of collagen, as recently demonstrated for Zn[14]. In addition, even when collagen is well preserved, combining traditional collagen $\delta^{15}N$ and $\delta^{13}C$ analyses with Zn isotope analyses of bioapatite may provide complementary dietary information as proven by the lack of correlation of those tracers within individuals of the same species, implying independent controlling mechanisms[15].

Nitrogen-15 becomes relatively enriched in the tissues of aquatic consumers with successive trophic level[16]. The $\delta^{13}C$ values behave much more conservatively with trophic level, increasing typically by less than 1 ‰ with trophic position for most tissues, compared to on average 3.4 ‰ higher $\delta^{15}N$ values between a predator and its prey[17,18]. Carbon isotopes are therefore more commonly used to infer the source(s) of primary production at the base of the food web. For Zn, studies have shown a distinct ^{66}Zn depletion in carnivore bioapatite relative to that of herbivores[11,14]. As muscles and most organs are typically ^{66}Zn depleted relative to the animal's diet and its bulk body $\delta^{66}Zn$ composition[19,20,21], bones of carnivores (and their bulk body composition) have lower $\delta^{66}Zn$ values than their prey's. Diet thus exerts control on the $\delta^{66}Zn$ values of soft tissue and bioapatite. Most non-diet related factors, such as sex and age of an animal, have so far shown no effect on the isotope values and relative isotopic variability in body tissues[21,22]. Provenance, on the other hand, appears to affect the Zn isotopic compositions of terrestrial vertebrates, though it remains unclear to which extent[11,14,23]. Provenance is known to play an important role for $\delta^{15}N$ and $\delta^{13}C$ studies in marine food webs[24] but has until now not been studied for $\delta^{66}Zn$.

In the marine realm, the $\delta^{15}N$ and $\delta^{13}C$ values of particulate organic matter (POM), consisting of phytoplankton, bacteria, microzooplankton and detritus, show a substantial spatial variation within and among ocean basins[5,25,26]. Variation in the isotopic composition at the base of the marine food web is passed along to higher trophic levels, limiting the comparability of populations from areas with varying isotopic food web baselines, or migratory animals. A high variability in modern baseline $\delta^{15}N$ and $\delta^{13}C$ values is documented by the isotopic composition of POM, zooplankton, filter feeders, as well as higher trophic level consumers across the Arctic[6,27,28,29,30,31] (Supplementary Text). Noteworthy is a west-east ^{13}C depletion observed in consumers from the Bering Sea (Bering Strait) through the Chukchi Sea to the Beaufort Sea[6,27,28,31] and significant spatial variability in zooplankton $\delta^{15}N$ and $\delta^{13}C$ values between the Canadian Arctic Archipelago (CAA), Labrador Sea, and Baffin Bay[31,32]. Particularly for bone collagen, with its long turnover time, trophic level reconstructions can be compromised when animals frequently

migrate between areas of differing baseline isotopic composition, or when comparing animals from spatially and temporally distinct locations.

Data on food web baseline δ^{66}Zn values and variability is non-existent for both the continental and marine realms. Because of biological uptake, dissolved Zn concentrations are highly depleted in marine surface waters, often much less than 1 nmol kg^{-1} [33,34]. The isotopic composition of dissolved Zn below 500 m seems to be globally homogenous with values close to +0.5 ‰, despite variable Zn concentrations[35,36]. Bulk marine Zn is enriched in ^{66}Zn relative to its major inputs from rivers and aeolian dust, which centre on the global crustal average of +0.3 ‰[37]. Although most studies on cultured phytoplankton demonstrate a preferential uptake of light Zn into the cell relative to the bulk growth medium[38,39], Atlantic and Pacific vertical Zn isotope profiles generally show lower δ^{66}Zn values in surficial waters compared to that of the deep water[33,36,40,41,42]. These studies demonstrate that the isotopic composition of Zn is most variable within the surface water (< 500 m), often with higher values in the uppermost surface (< 20 m).

Here, we aim at exploring Zn isotopes as a reliable tracer of marine trophic levels. To do so, we investigate combined bone δ^{66}Zn, δ^{15}N and δ^{13}C from the same species across 13 locations (17 sites) in a large geographic area stretching across the Arctic from the Hudson Strait in the east to the Bering Strait in the west. We include 5 locations and two single samples with already published δ^{15}N and δ^{13}C values[4,13,43,44], as well as one site with already published δ^{66}Zn values[13]. For this study, we analysed 167 archaeological bones, concentrating on polar bears (*Ursus maritimus*) and ringed seals *Pusa hispida* (*Phoca hispida*). Focusing on these species allows us to investigate δ^{66}Zn trophic level isotopic discrimination factors between predator and prey geographically. Both species have a circumpolar Arctic distribution and are abundant throughout the Arctic today[45,46]. Particularly, *P. hispida* remains are frequently found in archaeological assemblages with a large temporal and spatial range[43,47,48]. Studying the isotopic composition of high trophic level predators such as *U. maritimus* and *P. hispida* has the advantage of their tissues' composition dampening the effects of short-term environmental variation. This effectively leads to less isotopic variability and "noise" in the animal's tissues compared to those of lower trophic levels[43]. Therefore, these two species are prime targets to investigate geographical variability of dietary proxies and trophic level isotopic discrimination factors.

Results

Bone collagen δ^{13}C, δ^{15}N and bone δ^{66}Zn values of *P. hispida*, *U. maritimus*, harp seal (*Pagophilus groenlandicus*) and beluga whale (*Delphinapterus leucas*) are reported in table 1 and Supplementary Table 1. All collagen samples had yields and elemental (wt% C, wt% N, $C:N_{atomic}$) compositions characteristic of samples with isotopic compositions not altered by contaminant or degradation in the burial environment[49,50] (Supplementary Table 1). Likewise, δ^{66}Zn values do not indicate a modification due to diagenesis or contamination for the majority of samples, but we cannot exclude it as a possibility for outlier values (Supplementary Discussion). Our results also indicate that the presence of collagen-bound Zn and thereby collagen preservation has no effect on the mineral phase δ^{66}Zn values (Supplementary Fig. 1-2, Supplementary Table 2, Supplementary Results, Supplementary Discussion).

Statistically significant differences between *P. hispida* populations was determined through ANOVA for δ^{13}C ($F(12, 91) = 24.4$, *p-value* < 0.05), δ^{15}N ($F(12, 91) = 34.74$, *p-value* < 0.05) and δ^{66}Zn values ($F(12, 91) = 5.867$, *p-value* < 0.05). Post-hoc Tukey pair-wise comparisons draw out the populations from Little Cornwallis (QjJx-1) and the North shore of Devon Island (QkHn-13) both part of the CAA, as well as eastern

Ellesmere Island (near Skraeling Island, SfFk-4), linked to the North Water Polynya, as distinct from some of the other sites in regards to their δ^{66}Zn values (Extended Data Fig. 1). Every other site, regardless of their broad geographic group, are not significantly different from one another.

Results for pair-wise comparisons of sites' δ^{13}C and δ^{15}N *P. hispida* values show a higher degree of heterogeneity (Extended Data Fig. 2-3). However, most of the differences can be linked to geographic groups. Sites from the CAA are being drawn out as different in their δ^{13}C and δ^{15}N values to most of the other sites. The western sites of the Amundsen and Coronation Gulf, as well as the Bering Strait, differ in their δ^{15}N values, but not for δ^{13}C values. Finally, δ^{13}C and δ^{15}N values from the Eastern sites of the Hudson Bay and the Labrador Sea are identified as significantly different than those of western sites.

Levene's tests for equal variance show that δ^{66}Zn values are more homogeneous between *P. hispida* and *U. maritimus* ($F(1, 125) = 3.43$, $p = 0.27$) and across sites ($F(8, 118) = 1.72$, $p = 0.40$) than δ^{15}N values (respectively $F(1, 125) = 6.95$, $p = 0.04$; and $F(1,118) = 2.62$, $p = 0.05$).

Discussion

Site-specific isotopic variability

The maximum variability for inter-site mean *P. hispida* bone δ^{15}N and δ^{13}C values (3.55 and 3.40 ‰) exceeds the maximum intra-site (1.77 and 2.67 ‰, Fig. 1) and typical trophic level variability. The QjJx-1 site on Little Cornwallis Island is a notable exception with very high on-site *P. hispida* bone collagen δ^{15}N variability (3.85 ‰)[13]. Post-hoc Tukey pair-wise comparisons demonstrate a large heterogeneity in δ^{15}N and δ^{13}C values between archaeological populations (Extended Data Fig. 2-3). Isotopic heterogeneity between populations is related to geographic location resulting in δ^{15}N and δ^{13}C values from populations of different regions plotting in distinct groups on a δ^{15}N *versus* δ^{13}C plot (Fig. 1b). Based on site proximity and sample isotopic composition, we grouped sites from the Bering/Chukchi Sea, Amundsen and Coronation Gulf, CAA, North Water Polynya, Hudson Bay, and sites influenced by the Labrador Sea (Hudson Strait and Frobisher Bay, Fig. 1a). The δ^{15}N and δ^{13}C variability between the archaeological sites is in good agreement in both spacing and amplitude with modern geographical variations observed from zooplankton[26,27,28] and higher consumer soft tissue[6,27,28,31] including *P. hispida*[51,52,53,54,55,56] and *U. maritimus*[46]. While dietary differences between populations may have contributed to the geographic spacing of δ^{15}N and δ^{13}C values, an integration of regional baseline isotopic patterns is the main factor controlling the observed inter-site isotopic variability in *P. hispida* and *U. maritimus* collagen (Supplementary Discussion).

In contrast to *P. hispida* bone δ^{15}N and δ^{13}C values, the highest variability for mean δ^{66}Zn values between sites (0.23 ‰) does not exceed the maximum variability observed within a single site (0.36 ‰). Additionally, mean δ^{66}Zn values between sites never exceeds mean trophic position variability between *U. maritimus* and *P. hispida* (~0.32 ‰). While ANOVA analysis of *P. hispida* δ^{66}Zn values did reveal statistically significant differences between *P. hispida* populations, post-hoc pair-wise comparisons tests show considerably more homogeneity in δ^{66}Zn values than for δ^{15}N and δ^{13}C values (Extended Data Fig. 1-3). Similarly, Levene's tests for equal variance shows that for all sites, *P. hispida* and *U. maritimus* δ^{66}Zn values have an equal variance, whereas δ^{15}N values are more heterogeneous. The low geographical δ^{66}Zn

variability in *P. hispida* and *U. maritimus* bones implies that Arctic food-web baseline and/or low trophic level consumer δ^{66}Zn values are more homogenous than for δ^{15}N and δ^{13}C values. This is remarkable considering the large surface water's isotopic variability observed for dissolved Zn across the Atlantic and Pacific of −1.1 to +0.9 ‰ and −0.9 to +0.2 ‰, respectively[33,42].

Based on post-hoc Tukey pair-wise comparison, δ^{66}Zn values from *P. hispida* populations from the sites QjJx-1 (Little Cornwallis Island), QkHn-13 (Devon Island) and SfFk-4 (eastern Ellesmere Island) were identified as statistically different from other populations (Fig. 2, Extended Data Fig. 1). QjJx-1 and QkHn-13 are located within the CAA. The CAA is composed of multiple channels and interconnected basins, in which water mass modification and transport are governed by its complex topography and shelf exchange processes[57]. Within this setting, baseline δ^{66}Zn values may be more variable on a regional scale than for the rest of the Arctic. For the SfFk-4 site, we observe in all three species analysed lower mean δ^{66}Zn values compared to other sites indicating a regionally lower baseline δ^{66}Zn value (Fig. 2, Fig. 3). The SfFk-4 site is located at the biologically highly productive[58] northern edge of the North Water Polynya, a region in which the reduced ice-cover or ice-free conditions influence biological processes (e.g., by upwelling, increased nutrient renewal)[59], which in turn may modify the δ^{66}Zn baseline.

Species-specific isotopic variability

Both δ^{66}Zn and δ^{15}N values are controlled by diet but show a better correlation for *U. maritimus* samples across all sites than for *P. hispida* (Fig. 1 c, e), perhaps related to the more specialised diet of *U. maritimus*[60,61]. As with δ^{15}N values, bone δ^{66}Zn values clearly demonstrate a trophic spacing between *U. maritimus* and *P. hispida* in all locations analysed (Fig. 2). The KkJg-1 site in Hudson Bay is an exception with two *U. maritimus* samples showing anomalously high δ^{66}Zn values which may relate to non-dietary factors such as contamination, misidentification, diagenesis or physiological effects (Supplementary Discussion). Even when including the KkJg-1 site, Levene's tests for equal variance demonstrate an equal variance between *P. hispida* and *U. maritimus* δ^{66}Zn values ($F(1, 125) = 3.43$, $p = 0.27$), whereas their δ^{15}N values demonstrate heterogeneity ($F(1, 125) = 6.95$, $p = 0.04$). Because δ^{66}Zn is more homogenous in its value for a specific taxon (and diet?), δ^{66}Zn may more reliably reflect trophic positions than bulk δ^{15}N values, when investigating multiple species across multiple sites, proving a better inter-site comparability. *U. maritimus* bones are on average 0.32 ‰ lower than their primary prey species *P. hispida* (mean $\Delta^{66}Zn_{U. maritimus - P. hispida}$ = −0.32 ‰). Previously, estimations of trophic discrimination factors between enamel and bones of terrestrial mammalian carnivores and herbivores were between −0.6 and −0.4 ‰ for the Tham Hay Marklot (THM) cave[14] and the modern Koobi Fora region[11]. These studies, however, had a lower sample size and compared multiple carnivores and herbivores with varying diets. Predicted bone δ^{66}Zn trophic level discrimination factors are between −0.36 and −0.38 ‰ when calculated using individual δ^{15}N trophic levels[8] from all marine mammal taxa with available δ^{66}Zn data (Supplementary Discussion, Supplementary Equation 1-3). These values are close to the mean $\Delta^{66}Zn_{U. maritimus - P. hispida}$ value.

Particularly for archaeological material, assigning a trophic level to multiple species when utilising δ^{15}N values alone can be challenging, as shown by the large differences in mean δ^{15}N trophic discrimination factors between *U. maritimus* and *P. hispida* ($\Delta^{15}N_{U. maritimus - P. hispida}$) for individual sites (+2.2 to +7.0 ‰, Fig. 2 b). Besides diet, $\Delta^{15}N_{U. maritimus - P. hispida}$ variability may be influenced by physiological effects or

unknown archaeological assemblage effects related to human hunting and/or scavenging (Supplementary Discussion). For δ^{66}Zn, two sites from the same geographic area close to the Labrador Sea (KkDo-1 and JfEl-4), have a markedly lower trophic spacing between *P. hispida* and *U. maritimus* δ^{66}Zn values of −0.22 and −0.24 ‰ (Fig. 2). Modern *U. maritimus* individuals from the area belong to the Davis Strait population[62]. In addition to *P. hispida* and contrary to most other *U. maritimus* populations, this one obtains a large percentage of its biomass from the consumption of harp seals (*Pagophilus groenlandicus*)[60,61]. However, bone δ^{66}Zn of *P. hispida* and *P. groenlandicus* from the same site are indistinguishable (Fig. 3). Instead of the consumption of *P. groenlandicus*, the lower trophic discrimination factor for these sites may arise from unknown dietary contributions, population-specific physiological effects or unknown archaeological assemblage effects.

Unlike *P. hispida*, most *P. groenlandicus* leave their Canadian Arctic summering grounds, ahead of the formation of local pack ice in autumn[63,64]. However, when sympatric with *P. hispida*, *P. groenlandicus* feeds at a similar trophic level, consuming many of the same prey species, and both species show no statistical difference in muscle and liver δ^{15}N values[65]. Indeed, bones of both seal species cover the same δ^{66}Zn range for the same location (Fig. 3). However, bones of *P. groenlandicus* from Hudson Strait (KkDo-1) have almost 1 ‰ lower mean δ^{15}N and δ^{13}C values than those of *P. hispida*, perhaps related to this species' seasonal southwards migration (Fig. 3 b, d). In contrast, some *P. groenlandicus* individuals remain in west Greenland waters during winter[66,67], which may explain why bones of both seal species from eastern Ellesmere Island show a similar δ^{13}C, δ^{15}N and δ^{66}Zn range (Fig. 3 a, c). Due to its long turnover time, the bone collagen isotopic composition of *P. groenlandicus* likely represents an amalgamation of different food sources and local isotopic baseline values along their migration route and within their seasonal feeding grounds. *P. groenlandicus* bone δ^{66}Zn values do not seem to record migratory signals, again arguing for lower baseline variability or Zn isotopic homogenisation within low trophic level organisms. Despite a very low samples size (n = 2) beluga whale (*Delphinapterus leucas*) δ^{66}Zn values fall within the same range as *P. hispida* and *P. groenlandicus* with slightly higher mean values (Fig. 3b, d). Indeed, all three species occupy a similar trophic level[8,65]. When sympatric with *P. hispida*, *D. leucas* typically has slightly lower soft tissue δ^{15}N values likely due to migrating between areas with differing baselines or a more offshore/pelagic foraging[8,54]. Here, *D. leucas* δ^{15}N values are higher than those of *P. hispida* and their δ^{13}C values are highly variable (Fig. 3). Instead of only reflecting this species' trophic position relative to *P. hispida*, their collagen δ^{15}N and δ^{13}C values are likely influenced by the high mobility of this species[68] and its foraging in locations with different isotopic baselines.

The trophic levels of *U. maritimus*, *P. hispida* and *P. groenlandicus* are reflected by their bone collagen δ^{15}N and bone δ^{66}Zn values across the Arctic. The analysis of Zn isotopes, however, offers additional advantages for studying marine trophic ecology, not only due to its greater preservation potential in fossil material[14], but also due to the lower baseline controlled species-specific spatial isotopic gradients. The inclusion of δ^{66}Zn analysis in ecological, archaeological and palaeontological studies may thus allow more robust interpretations of spatial and temporal trophic interactions. Additionally, while both δ^{66}Zn and δ^{15}N generally record trophic levels, they do not record physiological and/or dietary effects equally, thus providing a strong incentive to combine δ^{66}Zn with δ^{15}N and δ^{13}C analyses where possible.

Conclusion

This study presents the first comparison of archaeological δ^{66}Zn bone compared with traditional collagen δ^{15}N and δ^{13}C values for the same species across a large geographic area. Focussing on prey (*P. hispida*) and predator (*U. maritimus*) we investigate the baseline variability and trophic spacing of these dietary proxies. Our results show that:

1) Overall, δ^{66}Zn values shows less site-specific variability within a species, likely due to a lower baseline variability than for δ^{15}N and δ^{13}C. As such, δ^{66}Zn values are particularly valuable for dietary studies on highly mobile species (or consumers thereof) and for comparing geographically and temporally distinct populations.
2) We observe the expected trophic level spacing for collagen δ^{15}N and bone δ^{66}Zn values between *U. maritimus* and *P. hispida*. *U. maritimus* bone δ^{66}Zn values are on average 0.32 ‰ lower than of its primary prey *P. hispida*.
3) Bone δ^{66}Zn values of the migratory species *P. groenlandicus* and *D. leucas* are consistent with respect to their known trophic positions when compared with *P. hispida* and *U. maritimus* values. In contrast, their collagen δ^{15}N (and δ^{13}C) values appear to document their relative trophic positions less precisely, likely influenced by variations in baseline isotopic compositions along their migration routes.

In ecological, archaeological and palaeontological research, trophic level estimations often rely exclusively on the δ^{15}N tracer, sometimes biased by physiological, habitat and baseline effects. We demonstrate that the inclusion of δ^{66}Zn analysis can provide otherwise inaccessible supplementary dietary information and more robust trophic level estimations.

Material and Methods

For this study, we compare δ^{66}Zn, δ^{15}N and δ^{13}C values of 104 *P. hispida*, 47 *U. maritimus*, 11 *P. groenlandicus* and 2 *D. leucas* archaeological bone samples from across the Arctic (Supplementary Table 1). The data presented herein includes already-published δ^{66}Zn values from an archaeological site (QjJx-1) on Little Cornwallis Island[13]. Additional δ^{66}Zn values analysed for this study comprise 93 *P. hispida* bone samples from 13 archaeological sites (12 locations) and 37 *U. maritimus* bone samples from 11 archaeological sites (8 locations) as well as *P. groenlandicus* and *D. leucas* samples (2 sites, 1 site, respectively). For 6 of the 17 sites analysed here (RbJu-1, PaJs-13, QkHn-13, QjJx-1, KTZ sites), δ^{15}N and δ^{13}C values were already published elsewhere[4,13,43]. Additionally, δ^{15}N and δ^{13}C values from one *P. hispida* sample from the NkRi-3 and OkRn-1 sites were already published elsewhere (Sample Nr. 4945, 9535)[44]. For the sites JfEl-4, KcFs-2, NkRi-3, seal bones analysed are identified as most likely *P. hispida*, but we cannot completely rule out that some samples may also come from other Phocidea (Supplementary Discussion). A single walrus (*Odobenus rosmarus*) bone and a potentially misidentified *D. leucas* bone from the JfEl-4 site were also measured and are discussed compared to previously measured *O. rosmarus* bones from the QjJx-1 site[13] and our δ^{66}Zn data from other species and sites in the Supplementary Discussion. Additional information and references regarding the archaeological context of the samples and sites are provided in the Supplementary Text.

δ^{66}Zn analysis

All samples' surfaces were mechanically abraded (cleaned) to avoid sediment contamination, using a dental drill equipped with a diamond-tipped burr. Approximately 10 to 50 mg chunks were then sampled using a diamond-tipped cutting wheel. The chunks were then ultrasonicated in ultrapure water (Milli-Q water) for 5 min and dried in a drying chamber for a few days at 50 °C. Bone samples and reference materials NIST SRM 1400 and NIST SRM 1486 were subjected to different dissolution methods (HCl and HNO_3) to investigate the impact of the organic bone phases on its Zn isotope signal (Supplementary Methods, Supplementary Discussion). The column chromatography steps (3.1.2) for a quantitative recovery of sample Zn[69,70] were the same for all samples regardless of the dissolution methods used. Each column chromatography batch (n = 15) included up to 13 samples, one chemistry blank and at least one reference standard (SRM 1400 and/or 1486).

Zn purification was performed in two steps, following the modified ion exchange method adapted from Moynier et al.[70], first described in Jaouen et al.[11]. Each step included AG-1x8 resin that was cleaned and conditioned prior to sample loading. One ml of AG-1x8 resin (200–400 mesh) was placed in 10 ml hydrophobic interaction columns (Macro-Prep® Methyl HIC). Resin cleaning involved 5 ml 3 % HNO_3 followed by 5 ml ultrapure water. These cleaning steps were repeated. The resin was then conditioned with 3 ml 1.5M HBr. After loading, 2 ml HBr were added for matrix residue elution followed by Zn elution with 5 ml HNO_3. Following the second column step, the solution was evaporated for 13 h at 100 °C and the residue re-dissolved in 1 ml 3 % HNO_3.

Zn isotope ratios were measured using a Thermo Fisher Neptune MC-ICP-MS at the Max Planck Institute for Evolutionary Anthropology (Leipzig, Germany) and a Thermo Fisher Neptune Plus MC-ICP-MS at the Géosciences Environnement Toulouse - Observatoire Midi-Pyrénées (Toulouse, France). Instrumental mass fractionation was corrected by Cu doping following the protocol of Maréchal et al.[69] and Toutain et al.[71]. The in-house reference material Zn AA-MPI was used for standard bracketing. δ^{66}Zn values are expressed relative to the JMC-Lyon reference material. Analysed sample solution Zn concentrations were close to 300 ppb as was the Zn concentration used for the standard mixture solution. Zn concentrations in the respective samples were estimated following a protocol adapted from one used for Sr by Copeland et al.[72], applying a regression equation based on the ^{64}Zn signal intensity (V) of three solutions with known Zn concentrations (150, 300 and 600 ppb). δ^{66}Zn uncertainties were estimated from standard replicate analyses and ranged between ± 0.01 ‰ and ± 0.03 ‰ (1SD). Additional reference materials SRM 1486 and SRM 1400 were analysed alongside the samples. SRM reference materials and samples show a normal Zn mass dependent isotopic fractionation, i.e. the absence of isobaric interferences, as the δ^{66}Zn vs. δ^{67}Zn and δ^{66}Zn vs. δ^{68}Zn values fall onto lines with slopes close to the theoretic mass fractionation values of 1.5 and 2, respectively.

δ^{13}C and δ^{15}N analysis

Bone surfaces were cleaned with a dental drill equipped with a diamond-cutting wheel. Subsamples of bone chunks (100-200 mg) were demineralised in 0.5 M HCl at 4°C. After demineralisation, samples were rinsed to neutrality with Type I water (resistivity >18.2 MΩ·cm). Any bone samples with dark colouration

were treated with 0.1 M NaOH for successive 30 min treatments under sonication at room temperature until the solution no longer changed colour. The samples rinsed to neutrality with Type I water and then the insoluble collagen residue was solubilised in ~8 ml of 0.01 M HCl at 75°C for 48 h. The resulting solution containing the solubilised collagen was filtered through a 5−8 µm filter and then filtered using a Microsep® 30 kDa molecular weight cut-off (MWCO) ultrafilter (Pall Corporation, Port Washington, NY) to remove low molecular weight compounds[73]. The >30 kDa fraction was freeze-dried, and the collagen yield was calculated.

Carbon and nitrogen isotopic and elemental compositions were determined using an IsoPrime continuous flow isotope-ratio mass spectrometer (CF-IRMS) coupled to a Vario Micro elemental analyser (Elementar, Hanau, Germany). Carbon and nitrogen isotopic compositions were calibrated relative to the VPDB and AIR scales, respectively, using a two-point calibration anchored by USGS40 (accepted $\delta^{13}C$ −26.39±0.04 ‰, $\delta^{15}N$ −4.52±0.06 ‰) and USGS41 (accepted $\delta^{13}C$ +37.63±0.05 ‰, $\delta^{15}N$ +47.57±0.11 ‰)[74]. Standard uncertainty was determined to be ±0.20 ‰ for $\delta^{13}C$ and ±0.25 ‰ for $\delta^{15}N$[75]. Additional details are provided in the Supplementary Methods.

Statistical analyses

Analysis of variance (ANOVA) were performed across the dataset in order to determine statistical differences in $\delta^{13}C$, $\delta^{15}N$ and $\delta^{66}Zn$ values between *P. hispida* populations. A single *P. hispida* specimen from Little Cornwallis Island was excluded from the statistical analysis ($\delta^{66}Zn$ = 1.00 ‰, from Jaouen et al.[13]), as it could disproportionately influence the analysis (see Extended Data Fig. 1-3 *versus* 4-6). It was singled-out as an extreme outlier lying more than 3 times the interquartile range above the third quartile, both within-site and for the whole *P. hispida* dataset. Where variance was found to be significant, post-hoc Tukey pair-wise comparisons were carried out to determine which populations were significantly different from each other in terms of their $\delta^{13}C$, $\delta^{15}N$ and $\delta^{66}Zn$ values. To adhere to ANOVA's assumptions, each *P. hispida* populations' $\delta^{13}C$, $\delta^{15}N$ and $\delta^{66}Zn$ datasets underwent visual inspection to check for normally distributed and homogeneous residuals, as well as tested for equal variance using Levene's test. Accordingly, we report the results of ANOVAs and post-hoc Tukey pair-wise comparisons (Extended Data Fig. 1-3). In order to investigate the homogeneity of $\delta^{66}Zn$ values within the Arctic relative to $\delta^{15}N$ values, a series of Levene's test for equal variance (with Bonferroni correction) was performed on Zn and N isotopic values between *P. hispida* and *U. maritimus*, as well as between sites for which data is available for both species. All statistical analyses were conducted using the free program R software[76].

References

1. Horstmann-Dehn, L., Follmann, E. H., Rosa, C., Zelensky, G. & George, C. Stable carbon and nitrogen isotope ratios in muscle and epidermis of arctic whales. *Mar. Mamm. Sci.* **28,** E173-E190 (2012).
2. Winder, M. & Schindler, D. E. Climate change uncouples trophic interactions in an aquatic ecosystem. *Ecology* **85,** 2100-2106 (2004).

3. Misarti N., Finney B. P., Maschner H. & Wooller M. J. Changes in northeast Pacific marine ecosystems over the last 4500 years: evidence from stable isotope analysis of bone collagen from archaeological middens. *Holocene* **19,** 1139-1151 (2009).
4. Szpak P., Buckley M., Darwent C. M. & Richards M. P. Long-term ecological changes in marine mammals driven by recent warming in northwestern Alaska. *Glob. Chang. Biol.* **24,** 490-503 (2018).
5. Michener, R. H. & Kaufman, L. *Stable isotope ratios as tracers in marine food webs: an update.* In: *Stable Isotopes in Ecology and Environmental Science,* (eds Michener, R. & Lajtha, K.), 238–282, (Oxford, 2007).
6. Dunton, K. H., Saupe, S. M., Golikov, A. N., Schell, D. M. & Schonberg, S. V. Trophic relationships and isotopic gradients among arctic and subarctic marine fauna. *Mar. Ecol. Prog. Ser.* **56,** 89-97 (1989).
7. Ramsay, M. A. & Hobson, K. A. Polar bears make little use of terrestrial food webs: evidence from stable-carbon isotope analysis. *Oecologia* **86,** 598-600 (1991).
8. Hobson, K. A. & Welch, H. E. Determination of trophic relationships within a high Arctic marine food web using $\delta^{13}C$ and $\delta^{15}N$ analysis. *Mar. Ecol. Prog. Ser.* **84,** 9-18 (1992).
9. Heuser, A., Tütken, T., Gussone, N. & Galer, S. J. Calcium isotopes in fossil bones and teeth − Diagenetic versus biogenic origin. *Geochim. Cosmochim. Acta* **75,** 3419-3433 (2011).
10. Martin, J. E., Vance, D. & Balter, V. Natural variation of magnesium isotopes in mammal bones and teeth from two South African trophic chains. *Geochim. Cosmochim. Acta* **130,** 12-20 (2014).
11. Jaouen, K., Beasley, M., Schoeninger, M., Hublin, J. J. & Richards, M. P. Zinc isotope ratios of bones and teeth as new dietary indicators: results from a modern food web (Koobi Fora, Kenya). *Sci. Rep.* **6,** 26281 (2016).
12. Martin, J. E., Tacail, T., Adnet, S., Girard, C. & Balter, V. Calcium isotopes reveal the trophic position of extant and fossil elasmobranchs. *Chem. Geol.* **415,** 118-125 (2015).
13. Jaouen, K., Szpak, P. & Richards, M. P. Zinc Isotope Ratios as Indicators of Diet and Trophic Level in Arctic Marine Mammals. *PLoS One* **11,** e0152299 (2016).
14. Bourgon, N. et al. Zinc isotopes in Late Pleistocene fossil teeth from a Southeast Asian cave setting preserve paleodietary information. *PNAS* **117,** 4675-4681 (2020).
15. Jaouen, K. What is our toolbox of analytical chemistry for exploring ancient hominin diets in the absence of organic preservation?. *Quat. Sci. Rev.* **197,** 307-318 (2018).
16. Minagawa, M. & Wada, E. Stepwise enrichment of ^{15}N along food chains: Further evidence and the relation between $\delta^{15}N$ and animal age. *Geochim. Cosmochim. Acta* **48,** 1135-1140 (1984).
17. Vander Zanden, M. J. & Rasmussen, J. B. Variation in $\delta^{15}N$ and $\delta^{13}C$ trophic fractionation: implications for aquatic food web studies. *Limnol. Oceanogr.* **46,** 2061-2066 (2001).
18. Post, D. M. Using stable isotopes to estimate trophic position: models, methods, and assumptions. *Ecology* **83,** 703-718 (2002).
19. Moynier, F., Fujii, T., Shaw, A. S. & Le Borgne, M. Heterogeneous distribution of natural zinc isotopes in mice. *Metallomics* **5,** 693-699 (2013).
20. Balter, V. et al. Contrasting Cu, Fe, and Zn isotopic patterns in organs and body fluids of mice and sheep, with emphasis on cellular fractionation. *Metallomics* **5,** 1470-1482 (2013).
21. Mahan, B., Moynier, F., Jørgensen, A. L., Habekost, M. & Siebert, J. Examining the homeostatic distribution of metals and Zn isotopes in Göttingen minipigs. *Metallomics* **10,** 1264-1281 (2018).

22. Jaouen, K. et al. Dynamic homeostasis modeling of Zn isotope ratios in the human body. *Metallomics* **11,** 1049-1059 (2019).
23. Jaouen, K. et al. Zinc isotope variations in archeological human teeth (Lapa do Santo, Brazil) reveal dietary transitions in childhood and no contamination from gloves. *PloS One* **15,** e0232379 (2020).
24. McMahon K. W., Hamady L. L. & Thorrold S. R. Ocean ecogeochemistry: A review. *Oceanogr. Mar. Biol.* **51,** 327-374 (2013).
25. Rau, G. H., Sweeney, R. E. & Kaplan, I. R. Plankton ^{13}C:^{12}C ratio changes with latitude: differences between northern and southern oceans. *Deep Sea Res. Part I Oceanogr. Res.* **29,** 1035-1039 (1982).
26. McMahon, K. W., Hamady, L. L. & Thorrold, S. R. A review of ecogeochemistry approaches to estimating movements of marine animals. *Limnol. Oceanogr.* **58,** 697-714 (2013).
27. Saupe, S. M., Schell, D. M. & Griffiths, W. B. Carbon-isotope ratio gradients in western arctic zooplankton. *Mar. Biol.* **103,** 427-432 (1989).
28. Schell, D. M., Barnett, B. A. & Vinette, K. A. Carbon and nitrogen isotope ratios in zooplankton of the Bering, Chukchi and Beaufort seas. *Mar. Ecol. Prog. Ser.* **162,** 11-23 (1998).
29. Tamelander, T., Kivimäe, C., Bellerby, R. G., Renaud, P. E. & Kristiansen, S. Base-line variations in stable isotope values in an Arctic marine ecosystem: effects of carbon and nitrogen uptake by phytoplankton. *Hydrobiologia* **630,** 63-73 (2009).
30. Pomerleau, C. et al. Spatial patterns in zooplankton communities across the eastern Canadian sub-Arctic and Arctic waters: insights from stable carbon ($\delta^{13}C$) and nitrogen ($\delta^{15}N$) isotope ratios. *J. Plankton Res.* **33,** 1779-1792 (2011).
31. Pomerleau, C. et al. Pan-Arctic concentrations of mercury and stable isotope ratios of carbon ($\delta^{13}C$) and nitrogen ($\delta^{15}N$) in marine zooplankton. *Sci. Total Environ.* **551,** 92-100 (2016).
32. De la Vega, C., Jeffreys, R. M., Tuerena, R., Ganeshram, R. & Mahaffey, C. Temporal and spatial trends in marine carbon isotopes in the Arctic Ocean and implications for food web studies. *Glob. Chang. Biol.* **25,** 4116-4130 (2019).
33. Conway, T. M. & John, S. G. The biogeochemical cycling of zinc and zinc isotopes in the North Atlantic Ocean. *Global Biogeochem. Cycles* **28,** 1111-1128 (2014).
34. Wyatt, N. J. et al. Biogeochemical cycling of dissolved zinc along the GEOTRACES South Atlantic transect GA10 at 40°S, *Global Biogeochem. Cycles* **28,** 44–56 (2014).
35. Sieber, M. et al. Cycling of zinc and its isotopes across multiple zones of the Southern Ocean: Insights from the Antarctic Circumnavigation Expedition. *Geochim. Cosmochim. Acta* **268**, 310-324 (2020).
36. Samanta, M., Ellwood, M. J., Sinoir, M. & Hassler, C. S. Dissolved zinc isotope cycling in the Tasman Sea, SW Pacific Ocean. *Mar. Chem.* **192,** 1-12 (2017).
37. Little, S. H., Vance, D., Walker-Brown, C. & Landing, W. M. The oceanic mass balance of copper and zinc isotopes, investigated by analysis of their inputs, and outputs to ferromanganese oxide sediments. *Geochim. Cosmochim. Acta* **125,** 673-693 (2014).
38. Samanta, M., Ellwood, M. J. & Strzepek, R. F. Zinc isotope fractionation by *Emiliania huxleyi* cultured across a range of free zinc ion concentrations. *Limnol. Oceanogr.* ***63*****,** 660-671 (2018).
39. Köbberich, M. & Vance, D. Zn isotope fractionation during uptake into marine phytoplankton: Implications for oceanic zinc isotopes. *Chem. Geol.* **523,** 154-161 (2019).

40. John, S. G. & Conway, T. M. A role for scavenging in the marine biogeochemical cycling of zinc and zinc isotopes. *Earth Planet. Sci. Lett.* **394,** 159-167 (2014).
41. Zhao, Y., Vance, D., Abouchami, W. & De Baar, H. J. Biogeochemical cycling of zinc and its isotopes in the Southern Ocean. *Geochim. Cosmochim. Acta* **125,** 653-672 (2014).
42. Liao, W. H. et al. Zn isotope composition in the water column of the Northwestern Pacific Ocean: the importance of external sources. *Global Biogeochem. Cycles* **34,** e2019GB006379 (2020).
43. Szpak, P., Savelle, J. M., Conolly, J. & Richards, M. P. Variation in late Holocene marine environments in the Canadian Arctic Archipelago: Evidence from ringed seal bone collagen stable isotope compositions. *Quat. Sci. Rev.* **211,** 136-155. (2019).
44. Szpak, P. & Buckley, M. Sulfur isotopes ($\delta^{34}S$) in Arctic marine mammals: Indicators of benthic vs. pelagic foraging? *Mar. Ecol. Prog. Ser.* http://doi.org/10.3354/meps13493 (2020).
45. Reeves, R. R. *Distribution, abundance and biology of ringed seals (Phoca hispida): an overview.* In: *Ringed Seals in the North Atlantic*, (eds Heide-Jørgensen, M. P. & Lydersen, C.) 9-45, (NAMMCO Scientific Publications, 1998).
46. Koehler, G., Kardynal, K. J. & Hobson, K. A. Geographical assignment of polar bears using multi-element isoscapes. *Sci. Rep.* **9,** 9390 (2019).
47. Moody, J. F. & Hodgetts, L. M. Subsistence practices of pioneering Thule–Inuit: A faunal analysis of Tiktalik. *Arctic Anthropol.* **50,** 4-24 (2013).
48. Dyke, A. S. et al. An assessment of marine reservoir corrections for radiocarbon dates on walrus from the Foxe Basin region of Arctic Canada. *Radiocarbon*, **61,** 67-81 (2019).
49. DeNiro M.J. Postmortem preservation and alteration of in vivo bone collagen isotope ratios in relation to palaeodietary reconstruction. *Nature* **317**, 806-809 (1985).
50. Ambrose, S. H. Preparation and characterization of bone and tooth collagen for isotopic analysis. *J. Archaeol. Sci.* **17,** 431-451 (1990).
51. Muir, D. C. G. et al. Can seal eating explain elevated levels of PCBs and organochlorine pesticides in walrus blubber from eastern Hudson Bay (Canada)?. *Environ. Pollut.* **90,** 335-348 (1995).
52. Hobson, K. A. et al. A stable isotope ($\delta^{13}C$, $\delta^{15}N$) model for the North Water food web: implications for evaluating trophodynamics and the flow of energy and contaminants. *Deep Sea Res. Part II Top. Stud. Oceanogr.* **49,** 5131-5150 (2002).
53. Young, B. G. & Ferguson, S. H. Seasons of the ringed seal: pelagic open-water hyperphagy, benthic feeding over winter and spring fasting during molt. *Wildl. Res.* **40,** 52-60 (2013).
54. Matley, J. K., Fisk, A. T. & Dick, T. A. Foraging ecology of ringed seals (*Pusa hispida*), beluga whales (*Delphinapterus leucas*) and narwhals (*Monodon monoceros*) in the Canadian High Arctic determined by stomach content and stable isotope analysis. *Polar Res.* **34,** 24295 (2015).
55. Dehn, L. A. et al. Feeding ecology of phocid seals and some walrus in the Alaskan and Canadian Arctic as determined by stomach contents and stable isotope analysis. *Polar Biol.* **30,** 167-181 (2007).
56. Butt, C. M., Mabury, S. A., Kwan, M., Wang, X. & Muir, D. C. Spatial trends of perfluoroalkyl compounds in ringed seals (*Phoca hispida*) from the Canadian Arctic. *Environ. Toxicol. Chem.* **27**, 542-553 (2008).
57. Michel, C., Ingram, R. G. & Harris, L. R. Variability in oceanographic and ecological processes in the Canadian Arctic Archipelago. *Prog. Oceanogr.* **71**, 379-401 (2006).
58. Tremblay, J. É., Gratton, Y., Carmack, E. C., Payne, C. D. & Price, N. M. Impact of the large-scale Arctic circulation and the North Water Polynya on nutrient inventories in Baffin Bay. *J. Geophys. Res.* **107,** 3112 (2002).

59. Ingram, R. G., Bâcle, J., Barber, D. G., Gratton, Y. & Melling, H. An overview of physical processes in the North Water. *Deep Sea Res. Part II Top. Stud. Oceanogr.* **49,** 4893-4906 (2002).
60. Iverson, S. J., Stirling, I. & Lang, S. L. C. *Spatial and temporal variation in the diets of polar bears across the Canadian Arctic: indicators of changes in prey populations and environment.* In: *Top predators in marine ecosystems*, (eds Boyd, I. L., Wanless, S. & Camphuysen, C. J.), 98–117, (Cambridge University Press, 2006).
61. Thiemann, G. W., Iverson, S. J. & Stirling, I. Polar bear diets and arctic marine food webs: insights from fatty acid analysis. *Ecol. Monogr.*, **78,** 591-613 (2008).
62. Lunn, N. J. et al. *Polar bear management in Canada 1997–2000*. In: *Proceedings of the 13th Working Meeting of the IUCN/SSC Polar Bear Specialist Group, 23–28 June 2001, Nuuk, Greenland. Occasional Paper 26,* (eds Lunn, N. J., Schliebe, S. & Born, E. W.), 41-52, (IUCN, 2002).
63. Ronald, K. & Dougan, J. L. The ice lover: biology of the harp seal (*Phoca groenlandica*). *Science* ***215***, 928-933 (1982).
64. Sergeant, D. E. Harp seals, man and ice. *Can. Spec. Publ. Fish. Aquat. Sci.* **114,** (1991).
65. Ogloff, W. R., Yurkowski, D. J., Davoren, G. K. & Ferguson, S. H. Diet and isotopic niche overlap elucidate competition potential between seasonally sympatric phocids in the Canadian Arctic. *Mar. Biol.* ***166*****,** 103 (2019).
66. Mansfield, A. W. Seals of arctic and eastern Canada. *Fish. Res. Board Canada Bull.* **137,** (1963).
67. Sergeant, D. E. Migrations of harp seals *Pagophilus groenlandicus* (Erxleben) in the Northwest Atlantic. *J. Fish. Res. Board Can.* **22,** 433-464 (1965).
68. Richard, P. R., Heide-Jørgensen, M. P., Orr, J. R., Dietz, R. & Smith, T. G. Summer and autumn movements and habitat use by belugas in the Canadian High Arctic and adjacent areas. *Arctic* **54,** 207-222 (2001).
69. Maréchal, C. N., Télouk, P. & Albarède, F. Precise analysis of copper and zinc isotopic compositions by plasma-source mass spectrometry. *Chem. Geol.* **156,** 251-273 (1999).
70. Moynier, F., Albarède, F. & Herzog, G. F. Isotopic composition of zinc, copper, and iron in lunar samples. . *Geochim. Cosmochim. Acta* **70,** 6103-6117 (2006).
71. Toutain, J. P. et al. Evidence for Zn isotopic fractionation at Merapi volcano. *Chem. Geol.* **253,** 74-82 (2008).
72. Copeland, S. R. et al. Strontium isotope ratios ($^{87}Sr/^{86}Sr$) of tooth enamel: a comparison of solution and laser ablation multicollector inductively coupled plasma mass spectrometry methods. *Rapid Commun. Mass Spectrom.* **22,** 3187-3194. (2008).
73. Brown T. A., Nelson D. E., Vogel J. S. & Southon J. R. Improved collagen extraction by modified Longin method. *Radiocarbon* **30,** 171-177 (1988).
74. Qi H., Coplen T. B., Geilmann H., Brand W. A. & Böhlke J. K. Two new organic reference materials for $\delta^{13}C$ and $\delta^{15}N$ measurements and a new value for the $\delta^{13}C$ of NBS 22 oil. *Rapid Commun. Mass Spectrom.* **17,** 2483-2487 (2003).
75. Szpak P., Metcalfe J. Z. & Macdonald R. A. 2017. Best Practices for Calibrating and Reporting Stable Isotope Measurements in Archaeology. *J. Archaeol. Sci. Rep.* **13,** 609-616 (2017).
76. R Core Team, *R version 3.6.1* (R Foundation for Statistical Computing, Vienna, Austria, 2018).

Acknowledgments

The Max Planck Society funded the cost of Zn isotope analyses and salary. P.S. was supported by the SSHRC Insight Development grant (grant number 430−2014−00046). Salary support was provided to K.J., P.M. and N.B. by the ERC ARCHEIS project (grant number 803676) and the DFG PALEODIET project (grant number 378496604). We thank S. Steinbrenner and M. Trost (Department of Human Evolution, Max Planck Institute for Evolutionary Anthropology, Leipzig) for technical support.

Author contributions

K.J. and J.M. designed the study. P.S., K.J. and J.M. selected the sample material. P.S., M.R. and C.H. performed the $\delta^{13}C$ and $\delta^{15}N$ analyses. J.M. and N.B. performed the $\delta^{66}Zn$ analyses at the MPI EVA Leipzig. J.M., K.J. and P.M. performed the $\delta^{66}Zn$ analyses at the CNRS in Toulouse. N.B. performed the statistical analysis. J.M., K.J., N.B., P.S., M.R. and J.-J.H., analysed and interpreted the data. J.M. wrote the initial manuscript. All authors contributed to editing the final version of the manuscript.

Competing interests

The authors declare no competing interests

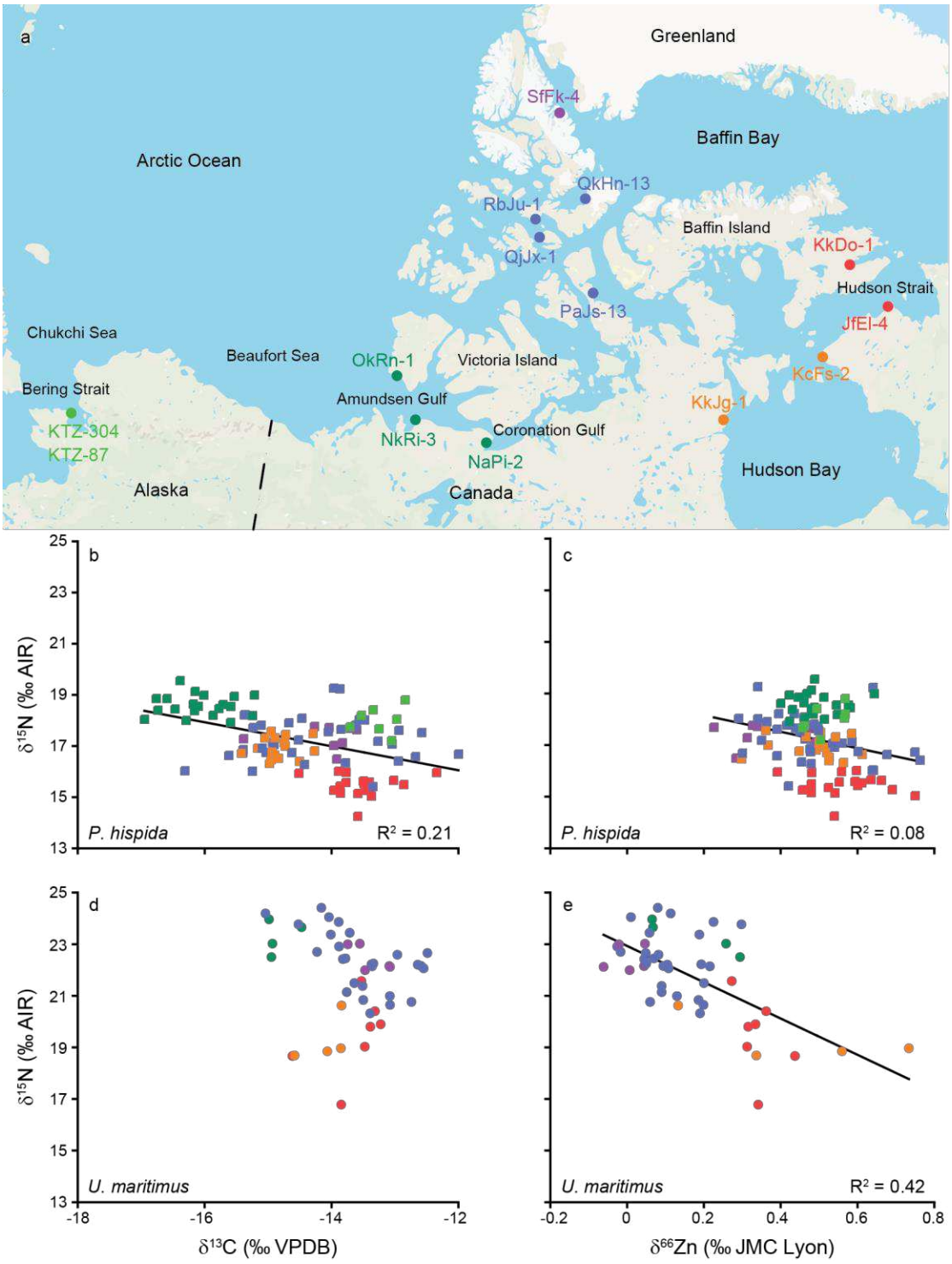

538

539 **Figure 1:** Isotopic composition of *P. hispida* (squares, n = 104) and *U. maritimus* (dots, n = 47) samples
540 from Arctic archaeological sites colour coded as geographic groups. a) Map indicating the archaeological
541 sites analysed and geographic colour coding: Light green for the Bering Strait; dark green for the
542 Amundsen and Coronation Gulf; blue for the CAA; orange for the Hudson Bay; purple for the North Water
543 Polynya; and red for sites influenced by the Labrador Sea in the Hudson Strait and Frobisher Bay. b) $\delta^{15}N$

versus $\delta^{13}C$ plot for *P. hispida* samples (*p-value* < 0.05; R^2 = 0.21; n = 104). c) $\delta^{15}N$ *versus* $\delta^{66}Zn$ plot for *P. hispida* samples (*p-value* < 0.05; R^2 = 0.08; n = 104). d) $\delta^{15}N$ *versus* $\delta^{13}C$ plot for *U. maritimus* samples (no correlation, *p-value* > 0.05; n = 47). e) $\delta^{15}N$ *versus* $\delta^{66}Zn$ plot for *U. maritimus* samples (*p-value* < 0.05; R^2 = 0.42; n = 47). We included already published $\delta^{15}N$ and $\delta^{13}C$ values[4,13,43,44] and already published $\delta^{66}Zn$ values from QjJx-1[13]. The map is redrawn after www.google.com/maps.

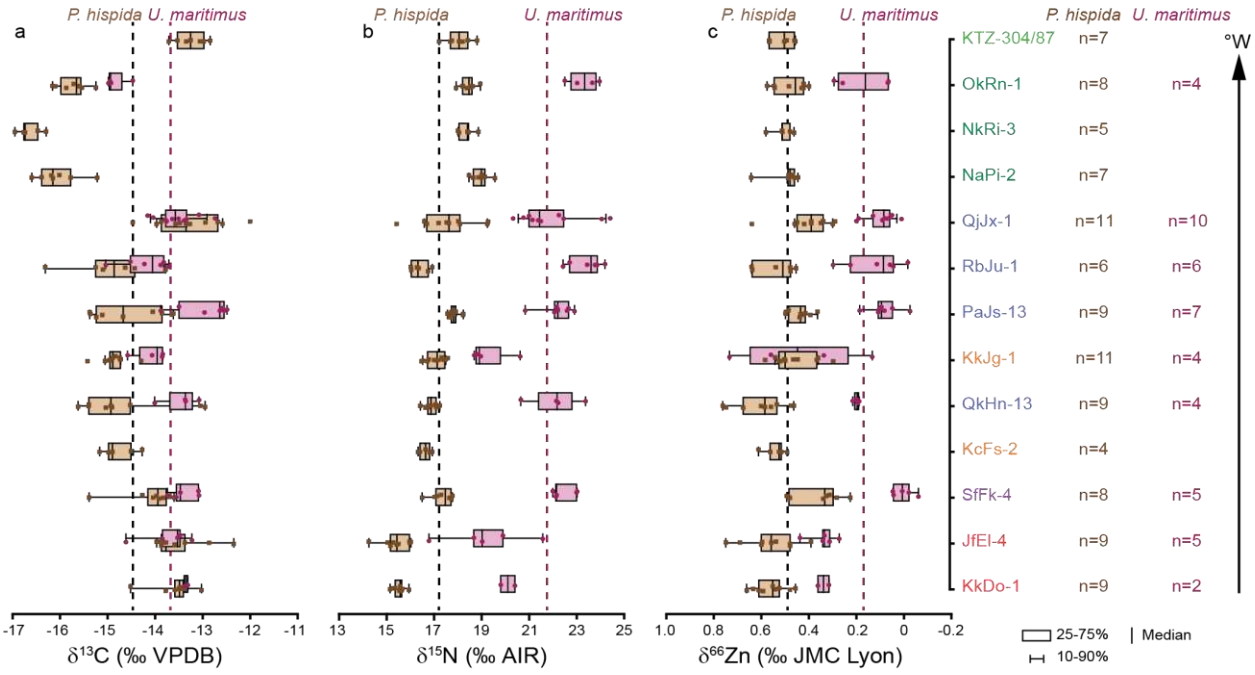

Figure 2: Range of $\delta^{13}C$ (a), $\delta^{15}N$ (b) and $\delta^{66}Zn$ (c) values for *P. hispida* and *U. maritimus* bones for all locations. Site names are colour coded following figure 1. Dashed lines represent mean values when including all sites. We included already published $\delta^{15}N$ and $\delta^{13}C$ values from sites RbJu-1, PaJs-13, QkHn-13, KTZ and QjJx-1 sites[4,13,43,44] and already published $\delta^{66}Zn$ values from QjJx-1[13].

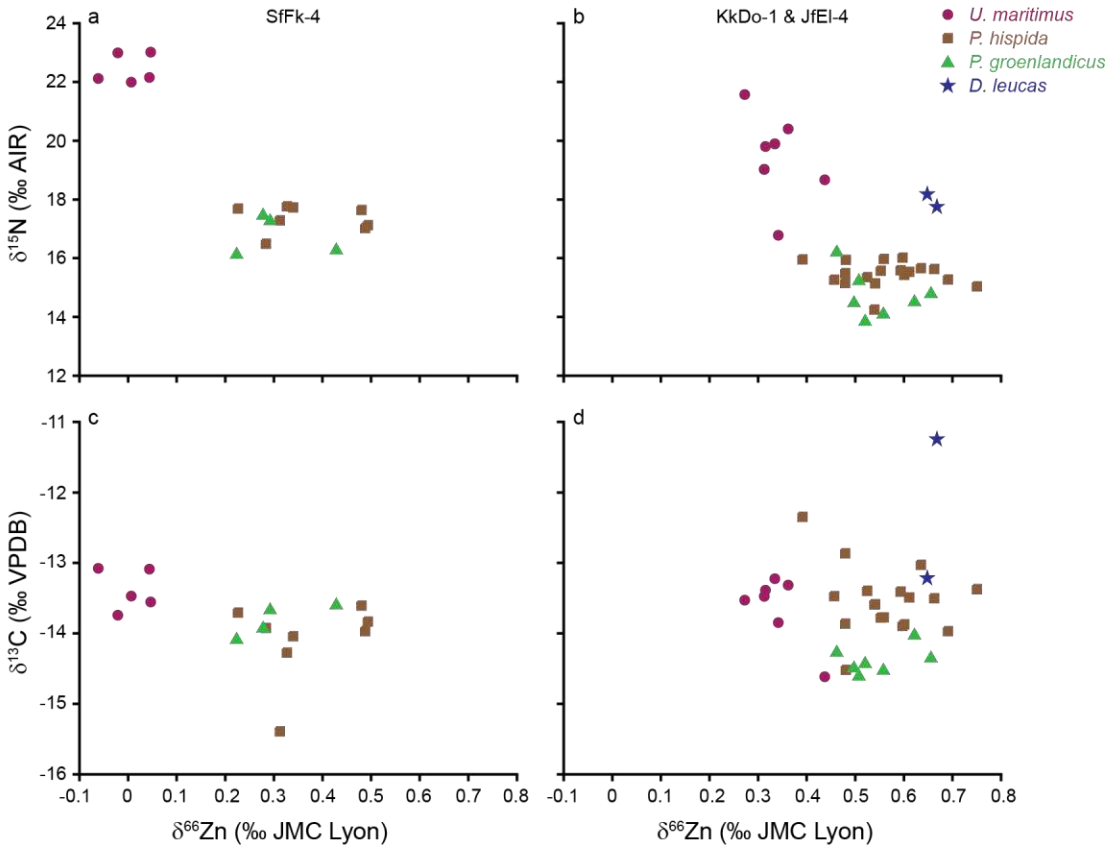

Figure 3: Isotopic composition ($\delta^{15}N$, $\delta^{13}C$ versus $\delta^{66}Zn$) of *U. maritimus* (dots), *P. hispida* (squares), *P. groenlandicus* (triangle) and *D. leucas* (star) bones for the SfFk-4 (a, c) and combined KkDo-1 and JfEl-4 sites (b, d).

570 **Table 1:** Isotopic range ($\delta^{13}C$, $\delta^{15}N$, $\delta^{66}Zn$) for all bone samples discussed in this study for which all three
571 elements were analysed. Max. = maximum value, min. = minimum value, SD = standard deviation, n =
572 number of individuals/bone samples, [Zn] Zn concentration.

Species	n		$\delta^{13}C$ (‰, VPDB)	$\delta^{15}N$ (‰, AIR)	$\delta^{66}Zn$ (‰, JMC Lyon)	[Zn] (µg/g)
U. maritimus	47	max.	−12.49	+24.41	+0.73	901
		min.	−15.04	+16.78	−0.06	80
		mean	**−13.68**	**+21.75**	**+0.17**	**276**
		SD	0.65	1.72	0.16	155
P. hispida	104	max.	−12.00	+19.56	+0.76	878
		min.	−16.95	+14.25	+0.23	79
		mean	**−14.48**	**+17.22**	**+0.49**	**167**
		SD	1.13	1.15	0.10	105
P. groenlandicus	11	max.	−13.60	+17.45	+0.66	273
		min.	−14.61	+13.84	+0.22	82
		mean	**−14.18**	**+15.47**	**+0.46**	**135**
		SD	0.35	1.26	0.14	57
D. leucas	2	max.	−11.24	+18.18	+0.67	1025
		min.	−13.21	+17.75	+0.65	381
		mean	**−12.23**	**+17.97**	**+0.66**	**703**
		SD	1.39	0.30	0.01	455

573

574

575

576

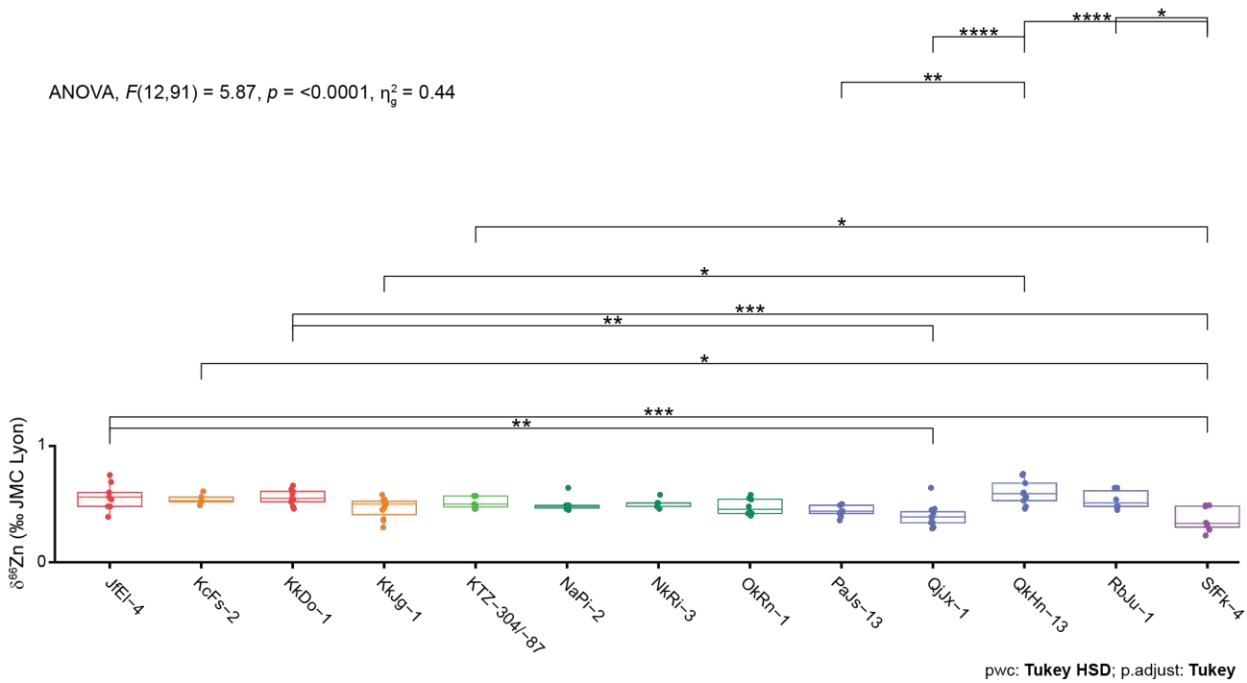

Extended Data Figure 1: Results for ANOVA testing and post-hoc Tukey pair-wise comparisons between sites (indicated by their Borden code) for δ^{66}Zn values of *P. hispida*. A single *P. hispida* specimen from Little Cornwallis Island[13] was excluded from statistical analysis as it was singled-out as an extreme outlier (δ^{66}Zn = 1.00 ‰). The boxes from the box and whisker plots represent the 25th–75th percentiles, with the median as a bold horizontal line. Significance level is indicated by "*" (*p-value* < 0.05), "**" (*p-value* < 0.005), "***" (*p-value* < 0.0005) and "****" (*p-value* < 0.00005).

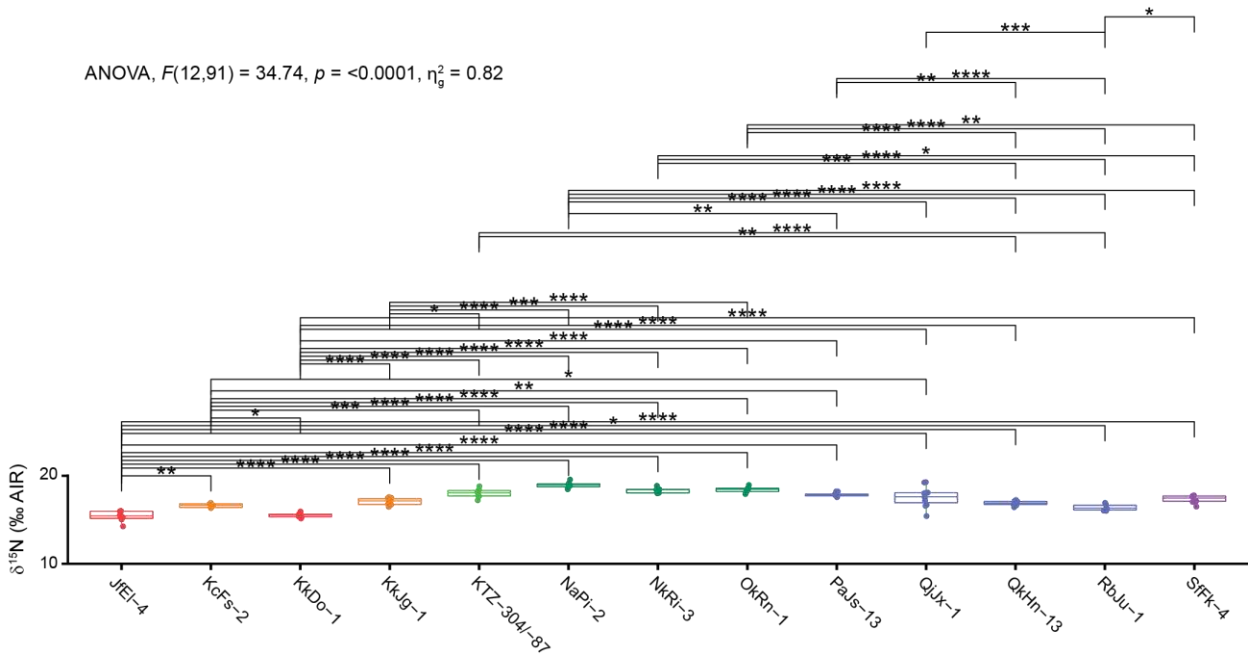

Extended Data Figure 2: Results for ANOVA testing and post-hoc Tukey pair-wise comparisons between sites (indicated by their Borden code) for $\delta^{15}N$ values of *P. hispida*. A single *P. hispida* specimen from Little Cornwallis Island[13] was excluded from statistical analysis as it was singled-out as an extreme outlier ($\delta^{66}Zn$ = 1.00 ‰). The boxes from the box and whisker plots represent the 25th–75th percentiles, with the median as a bold horizontal line. Significance level is indicated by "*" (*p-value* < 0.05), "**" (*p-value* < 0.005), "***" (*p-value* < 0.0005) and "****" (*p-value* < 0.00005).

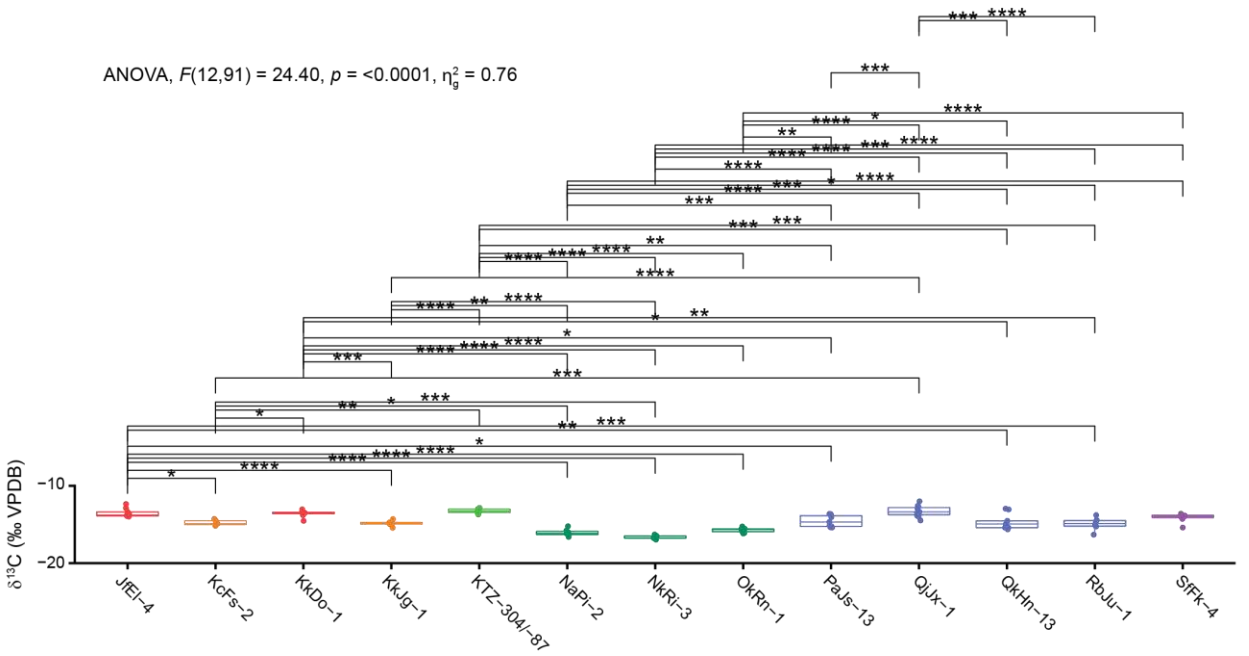

Extended Data Figure 3: Results for ANOVA testing and post-hoc Tukey pair-wise comparisons between sites (indicated by their Borden code) for $\delta^{13}C$ values of *P. hispida*. A single *P. hispida* specimen from Little Cornwallis Island[13] was excluded from statistical analysis as it was singled-out as an extreme outlier ($\delta^{66}Zn$ = 1.00 ‰). The boxes from the box and whisker plots represent the 25th–75th percentiles, with the median as a bold horizontal line. Significance level is indicated by "*" (*p-value* < 0.05), "**" (*p-value* < 0.005), "***" (*p-value* < 0.0005) and "****" (*p-value* < 0.00005).

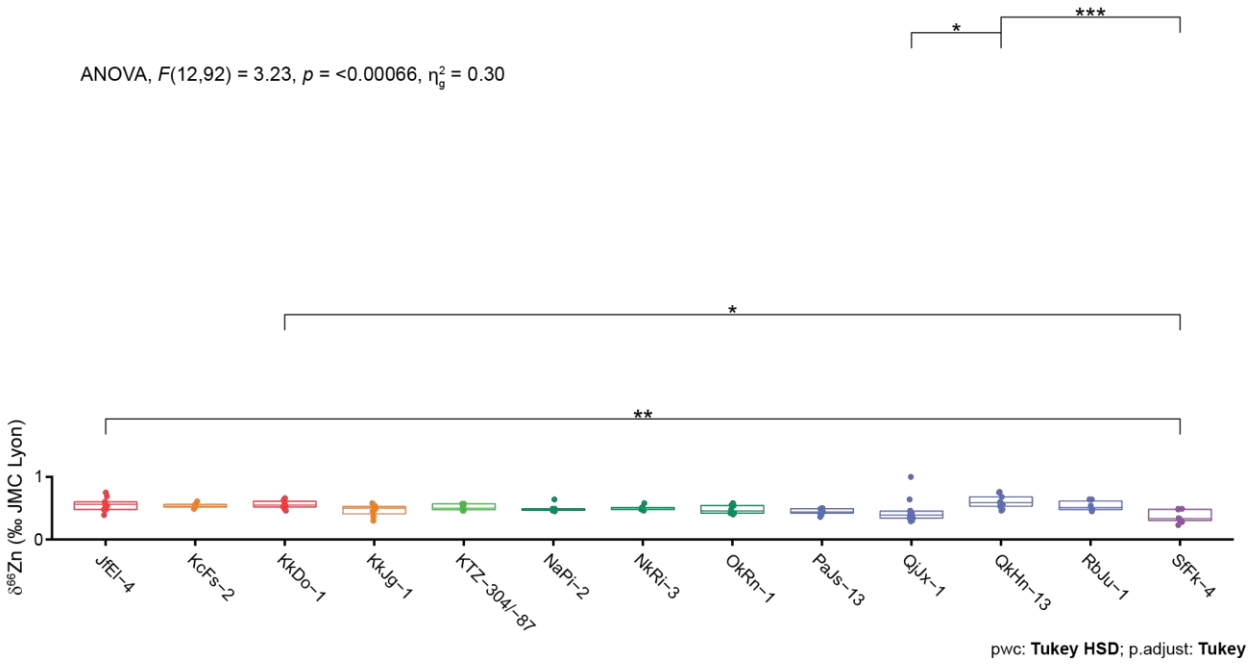

Extended Data Figure 4: Results for ANOVA testing and post-hoc Tukey pair-wise comparisons between sites (indicated by their Borden code) for δ^{66}Zn values of *P. hispida* including an extreme outlier value from Little Cornwallis Island[13]. The boxes from the box and whisker plots represent the 25th–75th percentiles, with the median as a bold horizontal line. Significance level is indicated by "*" (*p-value* < 0.05), "**" (*p-value* < 0.005), "***" (*p-value* < 0.0005) and "****" (*p-value* < 0.00005).

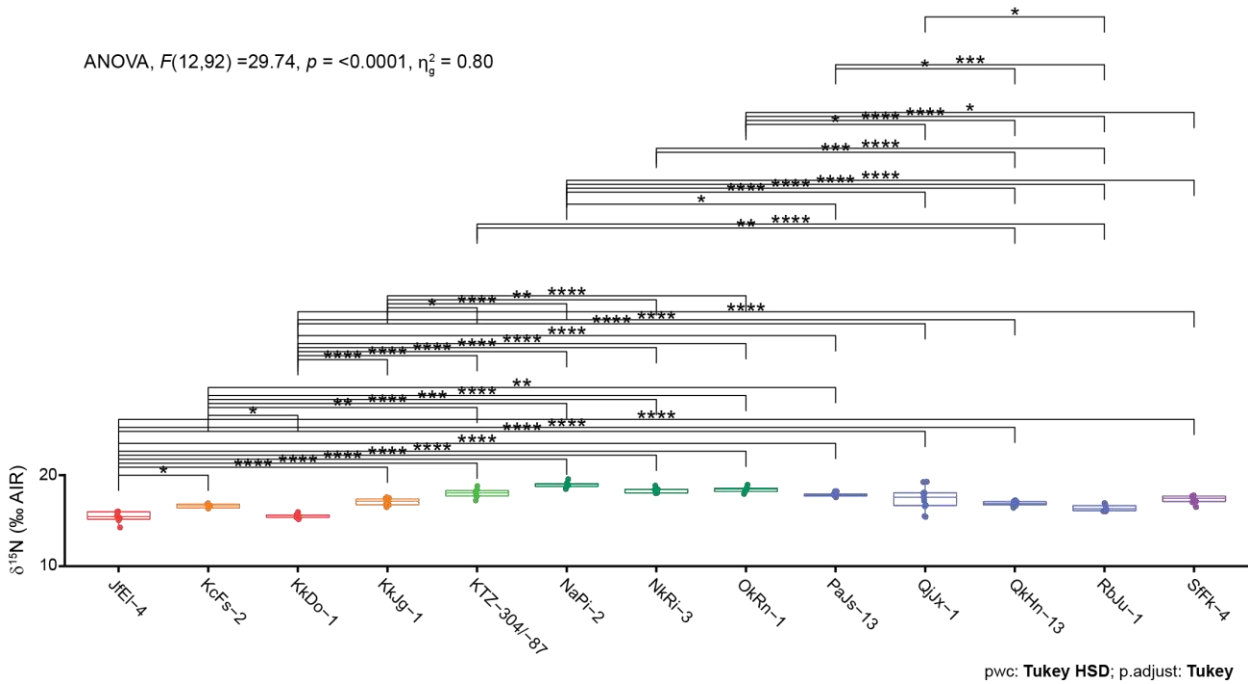

Extended Data Figure 5: Results for ANOVA testing and post-hoc Tukey pair-wise comparisons between sites (indicated by their Borden code) for δ^{15}N values of *P. hispida* including an extreme outlier value from Little Cornwallis Island[13]. The boxes from the box and whisker plots represent the 25th–75th percentiles, with the median as a bold horizontal line. Significance level is indicated by "*" (*p-value* < 0.05), "**" (*p-value* < 0.005), "***" (*p-value* < 0.0005) and "****" (*p-value* < 0.00005).

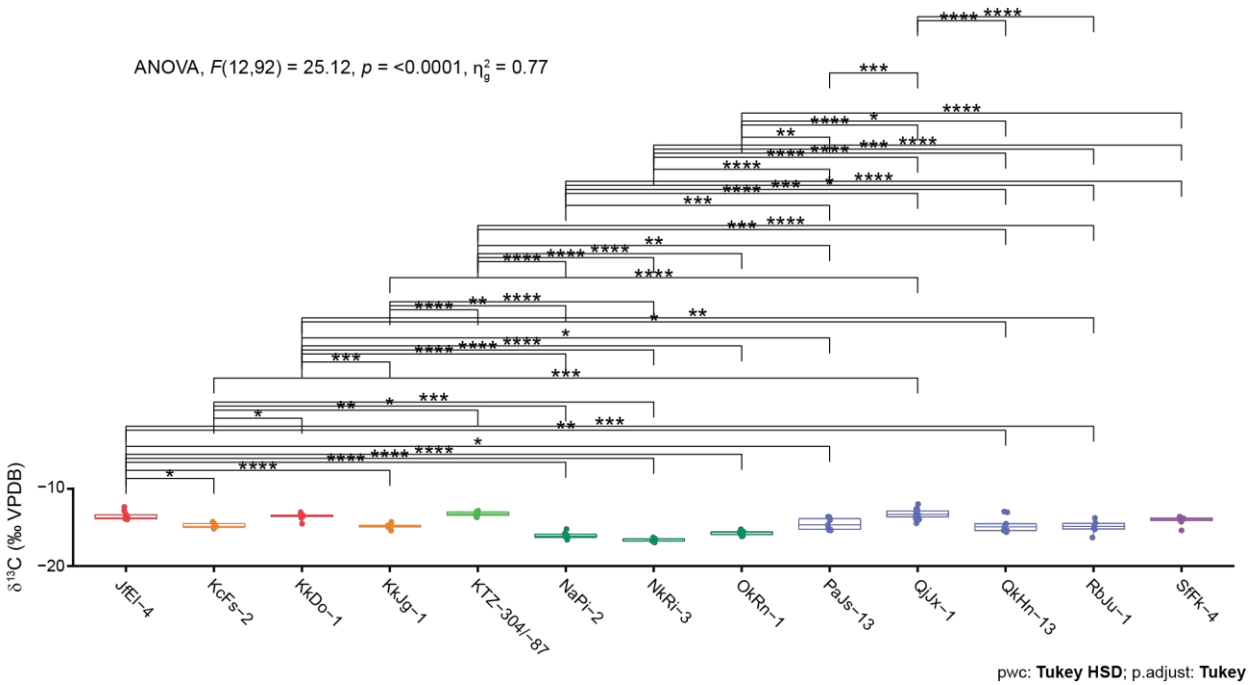

Extended Data Figure 6: Results for ANOVA testing and post-hoc Tukey pair-wise comparisons between sites (indicated by their Borden code) for $\delta^{13}C$ values of *P. hispida* including an extreme outlier value from Little Cornwallis Island[13]. The boxes from the box and whisker plots represent the 25th–75th percentiles, with the median as a bold horizontal line. Significance level is indicated by "*" (*p-value* < 0.05), "**" (*p-value* < 0.005), "***" (*p-value* < 0.0005) and "****" (*p-value* < 0.00005).

Figures

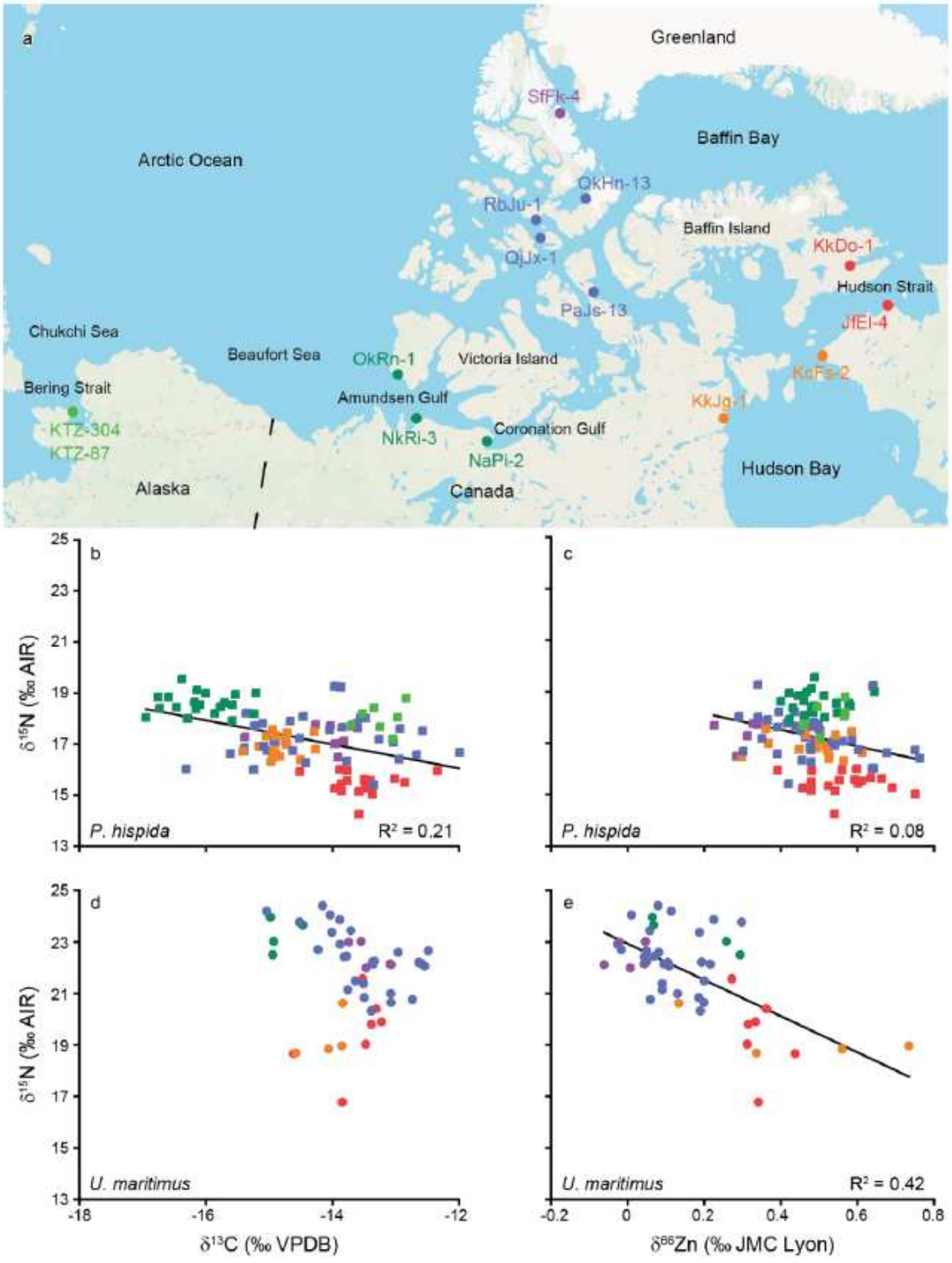

Figure 1

Isotopic composition of P. hispida (squares, n = 104) and U. maritimus (dots, n = 47) samples from Arctic archaeological sites colour coded as geographic groups. a) Map indicating the archaeological sites analysed and geographic colour coding: Light green for the Bering Strait; dark green for the Amundsen

and Coronation Gulf; blue for the CAA; orange for the Hudson Bay; purple for the North Water Polynya; and red for sites influenced by the Labrador Sea in the Hudson Strait and Frobisher Bay. b) δ15N versusδ13C plot for P. hispida samples (p-value < 0.05; R2 = 0.21; n = 104). c) δ15N versus δ66Zn plot for P. hispida samples (p-value < 0.05; R2 = 0.08; n = 104). d) δ15N versus δ13C plot for U. maritimus samples (no correlation, p-value > 0.05; n = 47). e) δ15N versus δ66Zn plot for U. maritimus samples (p-value < 0.05; R2 = 0.42; n = 47). We included already published δ15N and δ13C values4,13,43,44 and already published δ66Zn values from QjJx-113. The map is redrawn after www.google.com/maps. Note: The designations employed and the presentation of the material on this map do not imply the expression of any opinion whatsoever on the part of Research Square concerning the legal status of any country, territory, city or area or of its authorities, or concerning the delimitation of its frontiers or boundaries. This map has been provided by the authors.

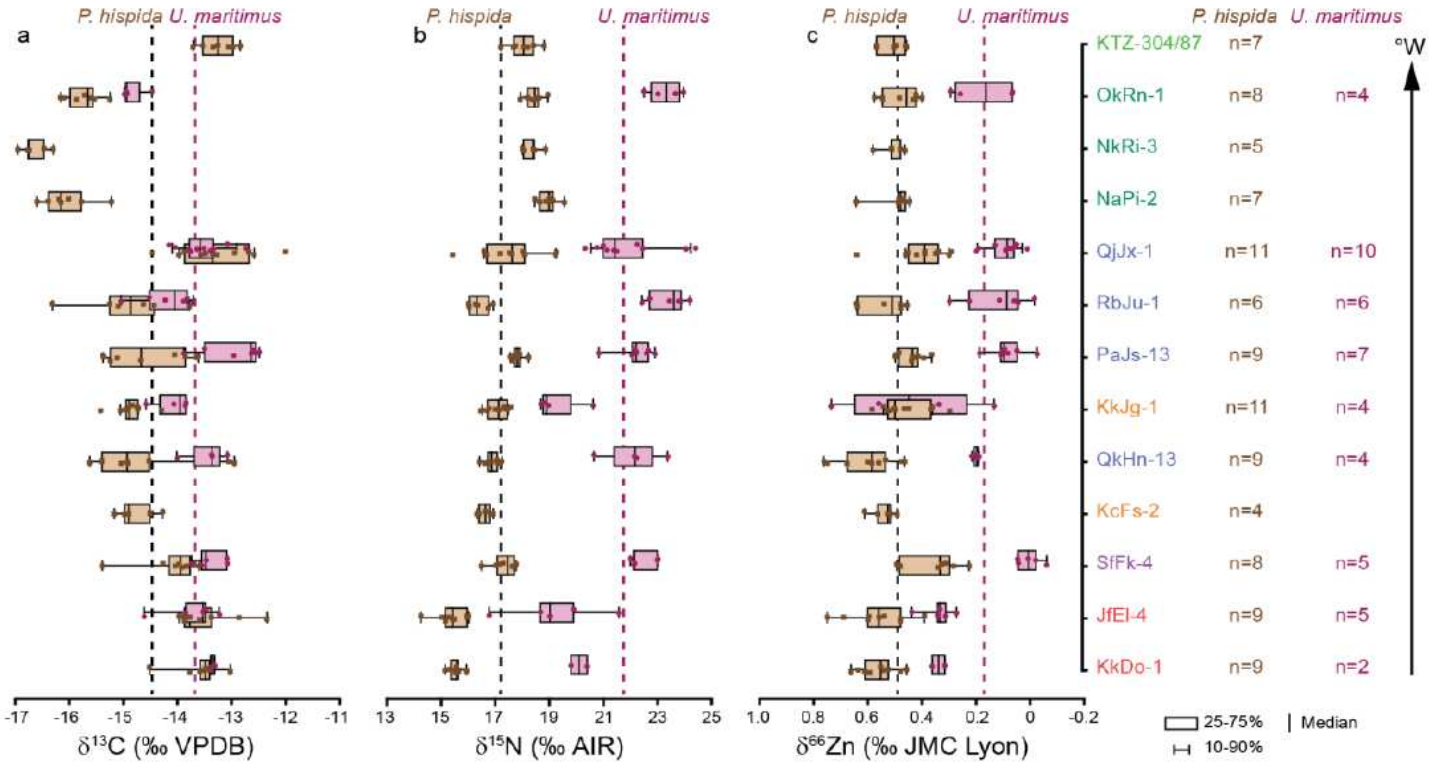

Figure 2

Range of δ13C (a), δ15N (b) and δ66Zn (c) values for P. hispida and U. maritimus bones for all locations. Site names are colour coded following figure 1. Dashed lines represent mean values when including all sites. We included already published δ15N and δ13C values from sites RbJu-1, PaJs-13, QkHn-13, KTZ and QjJx-1 sites4,13,43,44 and already published δ66Zn values from QjJx-113.

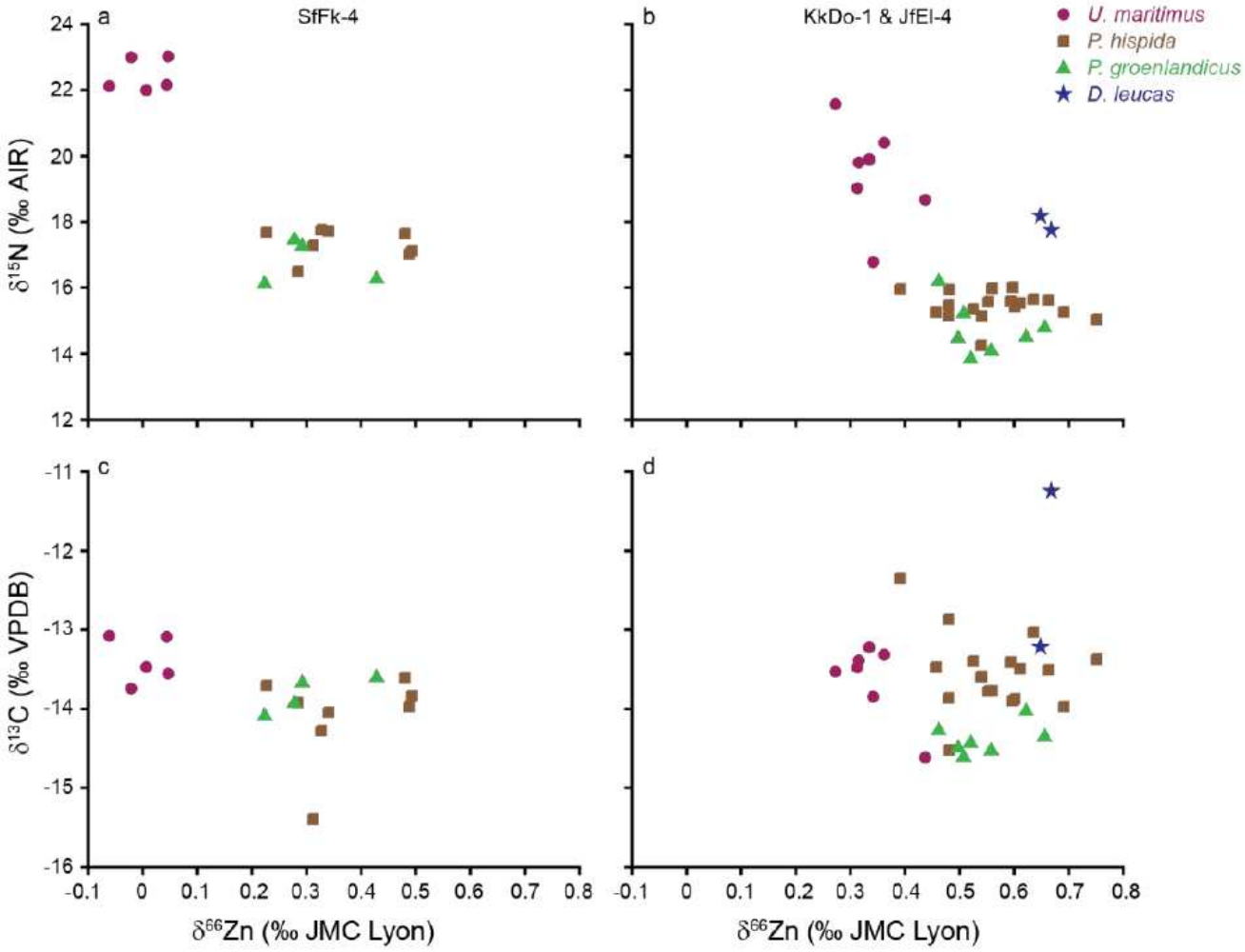

Figure 3

Isotopic composition (δ15N, δ13C versus δ66Zn) of U. maritimus (dots), P. hispida (squares), P. groenlandicus (triangle) and D. leucas (star) bones for the SfFk-4 (a, c) and combined KkDo-1 and JfEl-4 sites (b, d).

Supplementary Files

This is a list of supplementary files associated with this preprint. Click to download.

- SupplementaryInformationMcCormacketal.pdf
- SupplementaryTable1.xlsx
- SupplementaryTable2.xlsx